Assessment of the predictive capabilities of commercial simulation software packages for the analysis of the C redistribution during Q&P processing

T Klein[1], M Lukas[1], M Galler[2], and G Ressel[1]

[1] Materials Center Leoben Forschung GmbH, Roseggerstraße 12, 8700 Leoben, Austria

[2] voestalpine Wire Rod Austria GmbH, Drahtstraße 1, 8792 St. Peter Freienstein, Austria

E-mail: thomas.klein@mcl.at

Abstract. The C enrichment of austenite is of great importance to different kinds of transformation-induced plasticity-aided steels. Particularly, quenching and partitioning – a two-step heat treatment process, which involves the partial transformation to martensite and the subsequent C partitioning to austenite and its concomitant stabilization – has received considerable attention in recent years. The present work assesses the applicability of commercial software packages (DICTRA and MatCalc) to predict the interplay of C enrichment of austenite and concomitant C depletion of martensite. Results are additionally compared to calculations based on the "constrained carbon equilibrium" (CCE) and, moreover, to experiments conducted for two exemplary material conditions. DICTRA simulations extend the CCE calculation in terms of time dependence and allow to account for the possible displacement of the phase boundary, but lack the implications of the martensitic structure. Predictions based on MatCalc more accurately reflect experimental observations. Data gained allows for the evaluation of the predictive capabilities of commercial simulation packages corresponding to a prerequisite for the industrial implementation of novel heat treatment strategies and the required process control.

1 Introduction

The stabilization of considerable fractions of austenite via different processing routes is decisive to meet ductility requirements of advanced high strength steels (AHSS), which make use of the transformation-induced plasticity (TRIP) effect [1]. For this purpose, a suitable means is its stabilization via C enrichment by quenching and partitioning (Q&P) processing as originally introduced by Speer et al. [2], who derived a framework known as the "constrained carbon equilibrium" (CCE) for the calculation of the partitioning of C within a martensite/austenite assembly under given boundary conditions.

In the two-step Q&P process – a schematic representation of the heat treatment and the redistribution phenomena involved is shown in Figure 1 – the material is first cooled rapidly to the quenching temperature (T_Q) between martensite-start (M_s) and martensite-finish (M_f) temperatures allowing for the formation of martensite, whereby the temperature chosen allows adjusting a targeted martensite fraction. Subsequently, the material is isothermally heat treated at the

partitioning temperature ($T_P \geq T_Q$) for a duration t_p with the objective of C induced stabilization of the austenite, which can then be to a large extent retained to room temperature. The mechanism of C partitioning from martensite to austenite was recently corroborated using diffraction techniques [3], thermal analysis [4] and atom probe tomography [5]. Originally, the fundamental mechanisms of C escaping from a ferrite plate were discussed in the seminal works of Mujahid and Bhadeshia [6] and Hillert et al. [7] considering the C redistribution between austenite and ferrite following its displacive formation.

This study aims at comparing the predictive accuracy of state-of-the-art commercial software packages that allow for the calculation of the C redistribution during complex heat treatments. Gained data is compared to the classical CCE treatment as well as experimental results and discussed in the frame of current literature. Thereby, we aim at highlighting the strengths of thermodynamic and thermokinetic modelling techniques, which have become decisive for material and process development and their industrial implementation.

2 Materials and methodologies

In the present study, a low alloyed steel with nominal chemical composition of Fe-2.5Mn-1.5Si-0.2C (mass percent, m.%) was investigated. The material was delivered as sheets with 4 mm thickness, whereof cylindrical specimens were fabricated using electric discharge machining. Both heat treatments were conducted using a DIL 805 L/A dilatometer from TA Instruments according to the following scheme: Heating with a rate of 2 °C/s to an austenitization temperature of 900 °C, where the material was isothermally annealed for 1800 s followed by quenching with a rate of 10 °C/s to T_Q = 290 °C. After 10 s the material was reheated with a rate of 2 °C/s to T_P = 400 °C, where the isothermal partitioning heat treatment was conducted for 120 s or 600 s followed by final cooling to room temperature again with 10 °C/s.

Optical light microscopy (OLM) was performed using an Olympus BX51 microscope. Metallographic specimens were prepared by mechanical grinding and polishing followed by an etching procedure using Klemm 1 etchant. X-ray diffraction was performed using a Bruker AXS D8 Discover diffractometer with Mo-K_α radiation in Bragg-Brentano geometry. Phase fractions present were analyzed quantitatively using Rietveld refinement with the software package Topas version 5 from Bruker AXS. The austenite C concentration was evaluated from the empirical relationship suggested by Ruhl and Cohen [9] according to equation (1):

$$a_\gamma = 3.572 + 0.033w^C + 0.0012w^{Mn} - 0.00157w^{Si} \quad (1)$$

relating the austenite lattice constant a_γ to the concentrations of substitutional elements Mn and Si and the interstitially dissolved C each denoted by w^i given in m.%. The martensite C concentration was estimated based on the lever rule.

The thermokinetic calculations of the present study were conducted in DICTRA under the local equilibrium hypothesis [10] using tcfe8 (thermodynamic) and mobfe3 (mobility) databases and MatCalc 6.0 using Mc_fe.tdb v2.059 (thermodynamic) and Mc_fe.ddb v2.011 (mobility) databases. Results presented were obtained for isothermal annealing conditions at 400 °C using Fe-0.2C (m.%) model system similarly to the simplifications proposed by Seo et al. [11], who suggested that the slow partitioning of substitutional elements at 400 °C does not affect the redistribution of C. During partitioning the formation of cementite was disregarded and phase fractions were fixed. Additionally, the influence of dislocations in the martensitic structure on C concentrations was accounted for in MatCalc using the formulations of Refs. [12–14] assuming a fixed dislocation density, which is reasonable at 400 °C [15]. Calculations were conducted using Neumann boundary conditions, i.e. closed system scenarios. Additionally, the formulations according to Speer at al. [2], i.e. the CCE condition, was used to estimate and compare the C concentrations of the involved phases.

3 Results and discussion

3.1 Experimental results

Microstructure images taken by OLM of the material conditions investigated in the present work are depicted in Figure 2. (a) shows the microstructure after 120 s and (b) shows the microstructure after 600 s of partitioning heat treatment each at 400 °C. Blue and brown specimen regions correspond to martensite (α'), whereas white areas correspond to retained austenite (γ_R). Blocky retained austenite with dimensions up to ≈ 3 µm is discernible, while fine filmy austenite present in these material conditions may not be resolvable using OLM [11]. Visually no differences in microstructure between the two specimen conditions are observable using OLM.

The austenite phase fractions evaluated using Rietveld refinement of X-ray diffractograms are similar in both material conditions, f_γ(120 s) ≈ 9.7 m.% and f_γ(600 s) ≈ 9.8 m.%, i.e. appear not to diminish during an extended partitioning sequence. Upon increasing the partitioning duration an increase in austenite C concentration up to 1.2 m.% is discernible, which, however, remains clearly below the maximum value of ≈ 2.02 m.% given by full redistribution from martensite into austenite using the experimental phase fraction and austenite C concentration. Thus, a substantial amount of C is trapped at dislocations and interfaces of martensite and is, therefore, not available for stabilization of the retained austenite, which is a reasonable assumption according to e.g. Ref. [16].

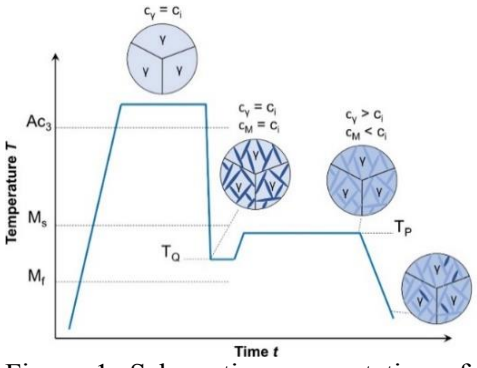

Figure 1. Schematic representation of the Q&P heat treatment and the evolution of C concentrations in the constituent phases redrawn according to Ref. [8].

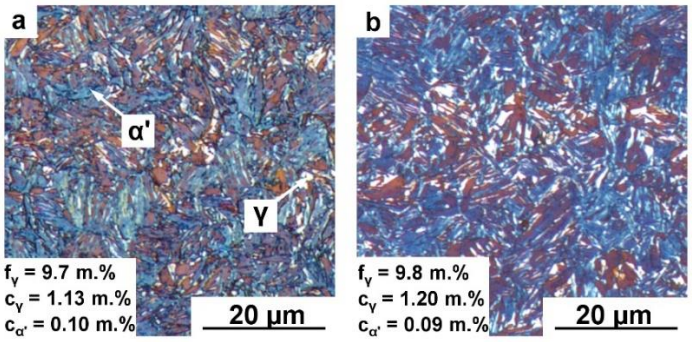

Figure 2. Microstructure images of the investigated Q&P material conditions of (a) t_p = 120 s and (b) t_p = 600 s. Apparently, morphology and phase fractions are hardly affected by the increased partitioning time, but slight variations of the C concentrations of the phases involved prevail.

3.2 Computational results

The kinetics of C redistribution across a martensite/austenite interface were calculated as depicted in Figure 3, where (a) and (b) show the DICTRA calculations and (c) and (d) correspond to the MatCalc calculations. Since C has a higher chemical potential in martensite than in austenite, the C concentration in ferrite is reduced during isothermal annealing at 400 °C [11]. Generally, the kinetics of C escaping from martensite are similarly predicted by both simulation approaches. The final concentration of the ferritic phase is obtained after 100 s using DICTRA at ≈ 0.003 m.% – a result that can be reproduced by MatCalc if trapping of C at dislocations is disregarded (see curve denoted by n.t. in (c)). If a dislocation density of 1×10^{15} m^{-3} is assumed comparing well with Ref. [15], the trapping of C inside the martensitic structure can be modelled successfully (c_α(100 s) ≈ 0.06 m.%), qualitatively matching well with the experimental results of the present work (c_α(120 s) ≈ 0.10 m.%) and literature (c_α(1000 s) ≈ 0.10 m.%) [3].

The enrichment of austenite by C, visible in Figure 3(b) and (d), shows slight discrepancies in terms of kinetics of C redistribution comparing the DICTRA and the MatCalc calculations. DICTRA predicts faster C redistribution (compare e.g. dotted lines corresponding to 1 s of partitioning). This discrepancy may result from the comparably high C concentration within the austenite at the beginning of the calculation using DICTRA in the direct vicinity of the interface to

martensite and the fact that the C diffusivity in austenite strongly depends on the C concentration [11]. Also, in (d) the effect of C trapping by dislocations in the ferritic phase is discernible. Diffusion profiles without trapping are labelled by n.t. Comparing the curves for 1 s partitioning time evidences that the kinetics of C redistribution are hardly affected, while the predictions for long partitioning durations differ dramatically in terms of maximum austenite C concentrations ($c_\gamma(100\text{ s})_{\text{n.t.}} \approx 1.98$ m.% and $c_\gamma(100\text{ s}) \approx 1.49$ m.%. This is due to the fact that a larger amount of C is available for austenite enrichment in the absence of trapping.

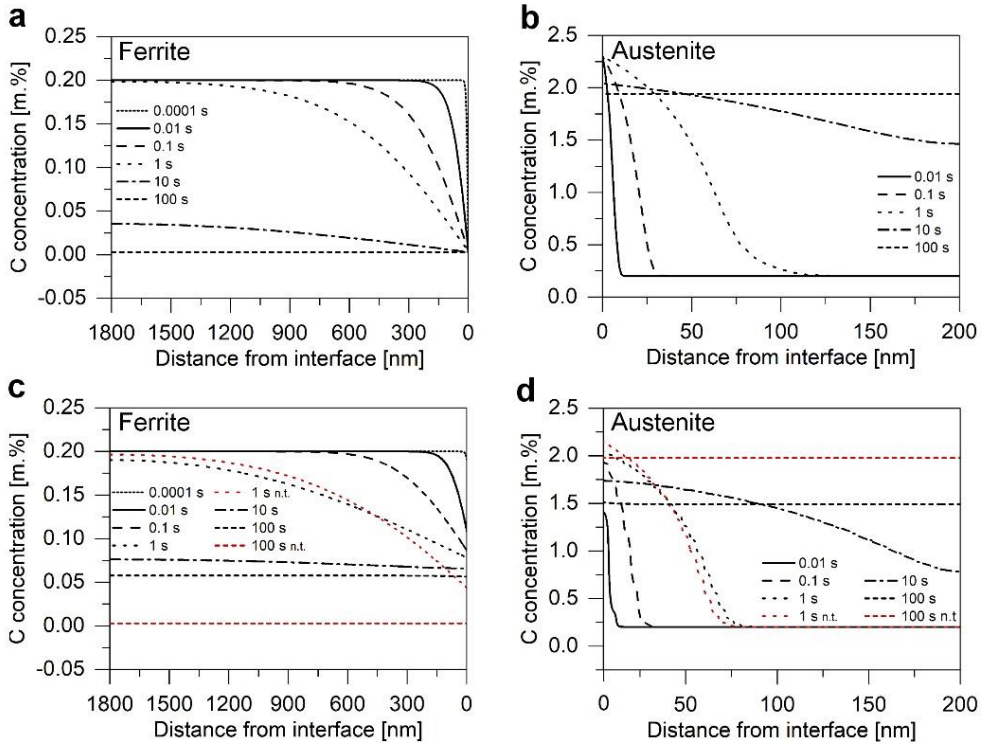

Figure 3. Results of the kinetic calculations of the C redistribution between ferrite and austenite during annealing at 400 °C. (a) and (b) correspond to DICTRA calculations, whereas (c) and (d) correspond to MatCalc calculations.

3.3 Comparison of experiment, kinetic calculations and CCE calculation

Results obtained by utilization of the CCE condition are depicted in Figure 4. Here, the C concentration in martensite (a) and austenite (b) are shown with respect to temperature for different martensite fractions. Comparing the values of the curve with a martensite fraction of 90% to the experimental results clearly shows that this calculation overestimates the C enrichment of austenite of $c_\gamma(600\text{ s}) \approx 1.20$ m.% in the investigated alloy and material condition, which is due to the fact that a non-negligible amount of C of about $c_\alpha(600\text{ s}) \approx 0.09$ m.% remains (inhomogeneously) in martensite. This effect can be accounted for in MatCalc as visualized in Figure 3(c). It should be mentioned that the differences between actual martensite C concentration of $c_\alpha(600\text{ s}) \approx 0.09$ m.% and the MatCalc prediction of $c_\alpha(100\text{ s}) \approx 0.06$ m.% may be rationalised by considering that by XRD a mean C concentration is determined averaging over different C concentrations present in tempered martensite and fresh martensite. Thus, the calculated C concentration is expected to closely match the C concentration of the tempered martensite.

The DICTRA calculations for long partitioning durations obtained in the present work resemble the concentrations predicted by the CCE condition (compare results of Figure 3(a) and (b) with the value the 90% martensite fraction curve depicted in Figure 4(a) and (b)). Moreover, these calculations fit well to the kinetic calculations performed by Seo et al. [11] using thermokinetic

simulation and Mecozzi et al. [17] using phase field simulation. The approach implemented in DICTRA, however, falls short of accurately modelling the complex structure of martensite and the resulting implications on C concentrations in both martensite and austenite. A suitable means to account for the actual implications of the martensitic structure is the physically well-founded treatment available in MatCalc based on Refs. [12–14], whereby the effect of the presence of dislocations is treated via their effect on the C chemical potential. The presence of these traps results in a reduction of the C chemical potential within ferrite. Since C redistribution stops once the C chemical potentials equal each other in martensite and austenite, i.e. no driving force for further diffusion is available, the equilibrium C concentration in martensite is increased in comparison to a defect free phase.

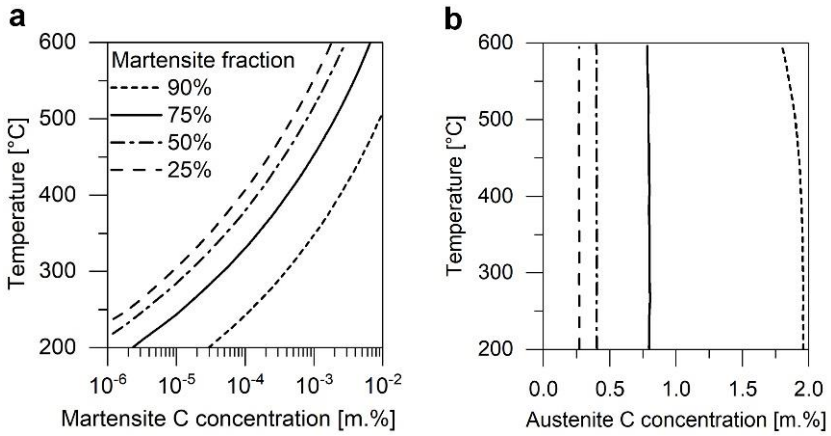

Figure 4. Dependence of (a) martensite C concentration and (b) austenite C concentration with respect to temperature for the Fe-0.2C (m.%) model system according to the CCE condition.

4 Summary and conclusion

The present work assesses the applicability of commercially available thermodynamic and thermokinetic software packages (DICTRA and MatCalc) to analyze the C enrichment of austenite and the depletion of martensite during a Q&P heat treatment. Moreover, two Q&P material conditions of a low alloyed steel are investigated experimentally. Results of kinetic calculations and experiments are compared to calculations based on the CCE condition and discussed in the frame of current literature. From the performed analyses the following conclusions can be drawn:

- Experiments conducted provide evidence for the enrichment of austenite with C during the partitioning heat treatment. The redistribution, however, clearly remains incomplete and a substantial amount of C is present within the martensite even after long partitioning heat treatment durations.
- DICTRA and MatCalc yield slightly differing kinetics of austenite C enrichment, which can be rationalised based on the dependence of the C diffusivity in austenite on the C concentration and differences in the boundary conditions applied.
- The effect of C trapping at dislocations within martensite can be accurately modelled using MatCalc resulting in increased C concentrations within martensite, while the kinetics are hardly affected.
- DICTRA calculations for long partitioning durations resemble estimations based on the CCE condition. Both generally overestimate the stabilization of austenite by C, whereas MatCalc calculations better approximate experimental results.

Acknowledgements

The authors gratefully acknowledge the financial support under the scope of the COMET program within the K2 Center “Integrated Computational Material, Process and Product Engineering (IC-

MPPE)" (Project No 859480). This program is supported by the Austrian Federal Ministries for Transport, Innovation and Technology (BMVIT) and for Digital and Economic Affairs (BMDW), represented by the Austrian research funding association (FFG), and the federal states of Styria, Upper Austria and Tyrol. The authors thank Y.V. Shan and Prof. Dr. E. Kozeschnik for fruitful discussions and support with the MatCalc calculations.

References

[1] Liu L, He B and Huang M X 2018 The Role of Transformation-Induced Plasticity in the Development of Advanced High Strength Steels *Adv. Eng. Mater.* **20** 1701083
[2] Speer J, Matlock D K, De Cooman B C and Schroth J G 2003 Carbon partitioning into austenite after martensite transformation *Acta Mater.* **51** 2611–22
[3] Clarke A J, Speer J G, Miller M K, Hackenberg R E, Edmonds D V, Matlock D K, Rizzo F C, Clarke K D and De Moor E 2008 Carbon partitioning to austenite from martensite or bainite during the quench and partition (Q&P) process: A critical assessment *Acta Mater.* **56** 16–22
[4] De Moor E, Föjer C, Penning J, Clarke A J and Speer J G 2010 Calorimetric study of carbon partitioning from martensite into austenite *Phys. Rev.* B **82** 1–5
[5] Toji Y, Matsuda H, Herbig M, Choi P P and Raabe D 2014 Atomic-scale analysis of carbon partitioning between martensite and austenite by atom probe tomography and correlative transmission electron microscopy *Acta Mater.* **65** 215–28
[6] Mujahid S A and Bhadeshia H K D H 1992 Partitioning of carbon from supersaturated ferrite plates *Acta Metall. Mater.* **40** 389–96
[7] Hillert M, Höglund L and Ågren J 1993 Escape of carbon from ferrite plates in austenite *Acta Metall. Mater.* **41** 1951–7
[8] Edmonds D V, He K, Rizzo F C, De Cooman B C, Matlock D K and Speer J G 2006 Quenching and partitioning martensite - A novel steel heat treatment *Mater. Sci. Eng.* A **438–440** 25–34
[9] Ruhl R and Cohen M 1969 Splat quenching of iron-carbon alloys *Trans. Met. Soc. AIME* **245** 241
[10] Borgenstam A, Engström A, Höglund L and Ågren J 2000 DICTRA, a Tool for Simulation of Diffusional Transformations in Alloys *J. Phase Equilibria* **21** 269–80
[11] Seo E J, Cho L and De Cooman B C 2016 Kinetics of the partitioning of carbon and substitutional alloying elements during quenching and partitioning (Q&P) processing of medium Mn steel *Acta Mater.* **107** 354–65
[12] Fischer F D, Svoboda J and Kozeschnik E 2013 Interstitial diffusion in systems with multiple sorts of traps *Model. Simul. Mater. Sci. Eng.* **21** 025008
[13] Svoboda J, Shan Y V, Kozeschnik E and Fischer F D 2013 Determination of depths of traps for interstitials from thermodynamic data: A new view on carbon trapping and diffusion *Model. Simul. Mater. Sci. Eng.* **21** 065012
[14] Svoboda J, Shan Y V, Kozeschnik E and Fischer F D 2014 Determination of depths of multiple traps for interstitials and their influence on diffusion kinetics *Model. Simul. Mater. Sci. Eng.* **22** 065015
[15] Kim B, Boucard E, Sourmail T, San Martín D, Gey N and Rivera-Diaz-del-Castillo P E J 2014 The influence of silicon in tempered martensite: Understanding the microstructure–properties relationship in 0.5 – 0.6 wt.% C steels *Acta Mater.* **68** 169–78
[16] Behera A K and Olson G B 2018 Nonequilibrium thermodynamic modeling of carbon partitioning in quench and partition (Q&P) steel *Scr. Mater.* **147** 6–10
[17] Mecozzi M G, Eiken J, Santofimia M J and Sietsma J 2016 Phase field modelling of microstructural evolution during the quenching and partitioning treatment in low-alloy steels *Comput. Mater. Sci.* **112** 245–56